Nonlinear Transport of the Wigner Solid on Superfluid ^{4}He in a Channel Geometry

Hiroki Ikegami,[1,2,*] Hikota Akimoto,[1] and Kimitoshi Kono[1]
[1]RIKEN, Hirosawa 2-1, Wako, Saitama 351-0198, Japan
[2]PRESTO, Japan Science and Technology Agency, Kawaguchi, Saitama 333-0012, Japan
(Received 17 November 2008; published 29 January 2009)

Nonlinear transport of electron crystal floating on superfluid ^{4}He is investigated in channels 8 and 15 μm in width, where the electron velocity and driving electric field are uniform. At a high excitation, we observe a jump in the velocity caused by the decoupling of the electrons from the underlying surface deformation. The obtained driving field at the jump indicates that the decoupling occurs from the dynamically deepened surface deformation as a result of the Bragg-Cherenkov scattering of surface waves. Our results also account for the unusual nonlinear transport reported by Glasson *et al.* [Phys. Rev. Lett. **87**, 176802 (2001)] considering the electrode geometry.

DOI: 10.1103/PhysRevLett.102.046807 PACS numbers: 73.50.Fq, 64.60.Cn, 67.90.+z, 73.20.−r

Two-dimensional electrons floating on the surface of superfluid ^{4}He form the best model system for strongly interacting electrons [1,2]. This system also provides a unique opportunity for investigating concerted effects between electrons and a soft interface. A number of distinct phenomena associated with the interaction with a free surface of liquid ^{4}He have been observed, in particular, in an electron crystal or the so-called Wigner solid (WS) phase, where electrons are self-trapped in commensurate surface deformation called the dimple lattice (DL).

The WS moves as a whole keeping the hexagonal lattice under a driving force parallel to the surface. An electron radiates surface waves (ripplons) when traveling faster than the ripplon phase velocity, as in the case of the Cherenkov radiation, and the ripplons emitted by different electrons interfere constructively if the wave number of the ripplons equals the reciprocal-lattice vector of the WS (the Bragg condition). This resonant Bragg-Cherenkov (BC) emission of ripplons gives rise to the limitation of the electron velocity, which was first observed by Kristensen *et al.* [3] and analyzed by Dykman and Rubo [4]. Another intriguing nonlinear phenomenon, a sharp rise in mobility at a much higher excitation, was found by Shirahama and Kono [5,6]. The rise was attributed to the decoupling of the WS from the DL, and the observed features were qualitatively understood by the decoupling from an undeformable rigid DL. Later, Vinen proposed, using a simple hydrodynamic model, that the decoupling occurs from the DL that deepens due to the BC scattering, and this bridges the two above-mentioned phenomena [7].

Although Vinen's model provides the qualitative picture of the decoupling mechanism from the BC state, its quantitative understanding is still poor because of the following difficulties in the experiments associated with the Corbino geometry, which has thus far been used for the studies of nonlinear transport. There, a large electron velocity distribution smears the nonlinear features. Moreover, the magnetic field, which is usually applied in Corbino experiments, makes the interpretation complicated owing to the presence of the shear elasticity in the WS phase [8,9]. For quantitative discussion of the decoupling mechanism, a study on a uniform electron velocity distribution in zero magnetic field is required.

In this Letter, we report the nonlinear transport of electrons confined in a channel under zero magnetic field. Owing to the uniform distributions of the electron velocity and the driving electric field along the channel, we can make quantitative arguments about the two important issues. First, we discuss the decoupling mechanism. The driving field required for the decoupling directly suggests that the decoupling occurs from the dynamically deepened DL as a result of the BC scattering. Next, we argue the unusual nonlinear transport reported by Glasson *et al.* [10]. We show that the unusual behavior they observed arises owing to the geometry they used.

Transport properties are investigated for electrons confined in channels 8 and 15 μm in width W using the device shown in Fig. 1(a). It is a double-layered structure with top and bottom electrodes made of an Al film separated by an insulating SiO_2 layer [Fig. 1(b)]. The bottom electrode consists of source, gate, and drain electrodes adjacent to each other with 100 nm gaps, which are positively biased with V_S, V_G, and V_D, respectively. The top electrode, called the guard electrode, has a pattern of the array of channels connected to each other, as shown in Fig. 1(a). The SiO_2 layer within the channels is removed to form the vertical groove, and it is filled with capillary-condensed liquid ^{4}He. Electrons are charged on the liquid surface and confined into the channels by a negative voltage applied to the guard electrode $V_{\rm guard}$.

The electrons located in the center channel form the quasi-one-dimensional conduction path (896 μm in length L for the 8 μm-wide channel). At both ends, the channel is connected to electron reservoirs, which are composed of the arrays of channels seen in the left and right parts of the device [Fig. 1(a)]. Thus, this system is schematically viewed as Fig. 1(c). Electrons in the reservoirs capacitively couple to the corresponding source or drain electrode. An

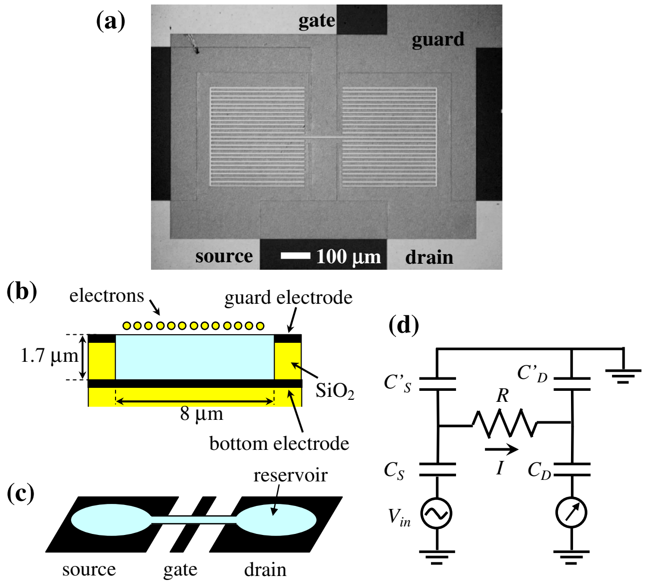

FIG. 1 (color online). (a) Device for the resistance measurement of the 8 μm-wide channel. (b) Schematic vertical cross section. The device is located 0.5 mm above the level of bulk liquid ^{4}He, and the channel is filled with the capillary-condensed liquid. (c) Schematic model of the system. (d) Lumped-constant circuit model. R is the resistance of the electrons in the center channel. C_S (C_D) represents the capacitance between the electrons and the source (drain), and C_S' (C_D') is that between the electrons and the guard.

ac voltage $V_{\rm in}$ applied to the source induces the current I in the center channel, and the induced current is detected by the drain. The velocity of electron v in the center channel is deduced from $v = I/(enW)$, where e is the elementary charge and n is the electron density. Because of the long center channel, this system can be modeled as the lumped-constant circuit shown in Fig. 1(d). The resistance R of the center channel is obtained by analyzing the detected current with this circuit, and the electric field $E_\parallel$ along the channel is deduced from $E_\parallel = RI/L$. Data presented here were obtained for $V_{\rm guard} = -0.10$ V and $V_S = V_D = V_G = +0.25$ V with $V_{\rm in}$ of 100 kHz. The electron density n is determined by the cutoff of the current when V_G is negatively biased with respect to V_S [10,11]. The electrons experience the holding field normal to the surface $E_\perp \simeq en/[\varepsilon_0(1+\varepsilon)]$, where ε_0 is the vacuum permittivity and ε is the relative permittivity of liquid ^{4}He. We performed the study for the 8 and 15 μm-wide channels and found essentially the same nonlinear behavior for both. In this Letter, we discuss only the results obtained for the 8 μm-wide channel.

The advantage of the long channel geometry is the uniform distributions of v and $E_\parallel$. It was confirmed by simulating the distribution of current in a linear regime by taking into account the pattern of the reservoir channels [12]. The simulation for the 8 μm-wide channel shows that v and $E_\parallel$ are uniform within 5% along the center channel. It also indicates that the resistance obtained by assuming the lumped-constant circuit [Fig. 1(d)] is only 1.04 times larger than the actual resistance, proving the validity of this circuit analysis.

Figure 2 shows R as a function of temperature T for the 8 μm-wide channel. In the electron gaseous phase at high temperatures, R decreases with lowering T, and closely follows the theory in which the mobility is limited by scattering with helium vapor atoms and ripplons [13], if the theoretical R is multiplied by a factor of 1.15. This factor is slightly larger than the value due to the above-mentioned simulation (1.04), but it indicates that the absolute value of R is accurate within about 10%. With a further decrease in temperature, the WS transition occurs at the temperature $T_m^{\rm 2D}$ when the plasma parameter becomes around 130 [1]. Below $T_m^{\rm 2D}$, a strong excitation dependence of R is observed. Particularly for $V_{\rm in} \leq 8.0$ mV$_{\rm rms}$, R drastically increases due to the BC scattering, as discussed below.

Figures 3(a)–3(c) show the excitation dependences of R, v, and $E_\parallel$ in the WS phase. The linear transport region is not seen even at small $V_{\rm in}$. R drastically increases with $V_{\rm in}$, followed by a sharp drop at $V_{\rm in}^{\rm th}$. At $V_{\rm in} < V_{\rm in}^{\rm th}$, v exhibits a clear plateau, as seen in the inset of Fig. 3(b). The plateau extends to a higher $V_{\rm in}$ at a lower T. The slight tilt of the plateau is due to the systematic error in the current measurements at such a high resistance. At $V_{\rm in}^{\rm th}$, v jumps to a much higher value, accompanied by a sharp drop in R. The transition is sharp at low temperatures, while it is smeared near $T_m^{\rm 2D}$.

The velocity at the plateaus is close to the ripplon phase velocity $v_1 = \omega(\mathbf{G_1})/|\mathbf{G_1}| = 6.9$ m/s at the first reciprocal-lattice vector $\mathbf{G_1}$ [dashed line in the inset of Fig. 3(b)], where $\omega(\mathbf{q})$ is the angular frequency of the ripplon with a wave vector $\mathbf{q}$. This fact proves that the BC scattering occurs in the plateau region [3,4]. Many

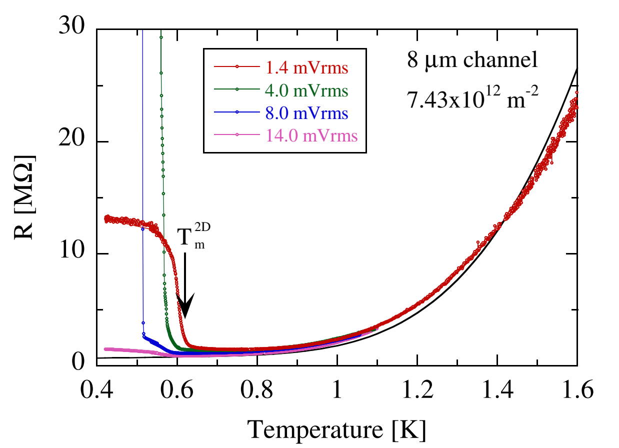

FIG. 2 (color online). Temperature dependence of R of the 8 μm-wide channel for $V_{\rm in} = 1.4$, 4.0, 8.0, and 14.0 mV$_{\rm rms}$. The arrow indicates the melting temperature of the WS (the plasma parameter is 130). The solid line indicates the resistance calculated from the theoretical mobility [13] for $E_\perp = 6.5 \times 10^4$ V/m, multiplied by a factor of 1.15.

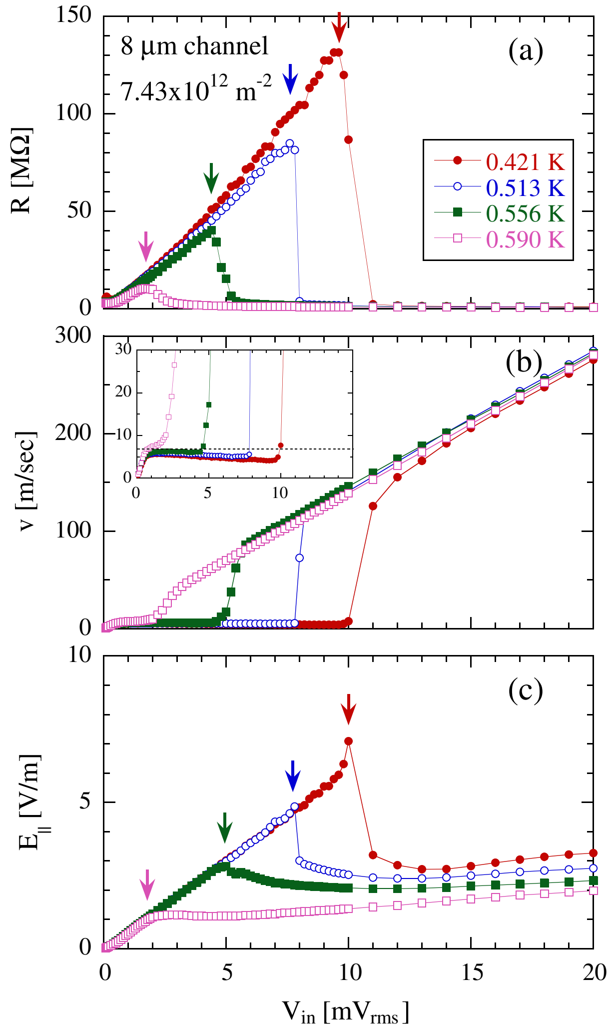

FIG. 3 (color online). V_{in} dependences of (a) R, (b) v, and (c) $E_{\parallel}$ in the WS phase. Arrows in (a) and (c) indicate $V_{\mathrm{in}}^{\mathrm{th}}$ and $E_{\parallel}^{\mathrm{th}}$, respectively. The inset of (b) is the expanded view of the low-velocity region. The dashed line indicates v_1.

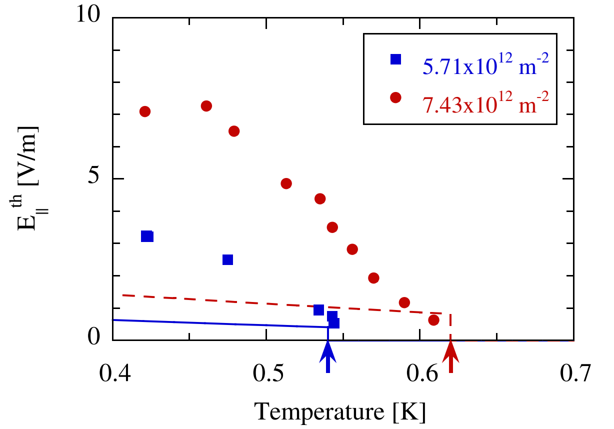

FIG. 4 (color online). Temperature dependence of $E_{\parallel}^{\mathrm{th}}$. Solid line and dashed line represent $E_{\mathrm{rigid}}^{\mathrm{th}}$ for $n = 5.71 \times 10^{12}$ and 7.43×10^{12} m^{-2}, respectively (see text). Arrows indicate T_m^{2D}.

ripplons are emitted by different electrons, and these ripplons with a wave vector $\mathbf{G}_1$ interfere constructively. The emission rate increases divergently as v approaches v_1, setting the upper limit on v. This process makes the dimple deeper resonantly, resulting in the strong increase of the frictional force acting on the DL [9], and thus the observed increase in $E_{\parallel}$.

At V_{th}, the BC state finally breaks into the high-velocity state due to the strong driving field $E_{\parallel}^{\mathrm{th}}$ [Fig. 3(c)]. This is caused by the collective decoupling of the electrons from the underlying DL. The DL disappears and the decoupled WS moves as a whole with a velocity much higher than v_1 [14].

Figure 4 shows the threshold field $E_{\parallel}^{\mathrm{th}}$ as a function of T. $E_{\parallel}^{\mathrm{th}}$ continuously decreases with increasing T and smoothly vanishes at T_m^{2D}. This smooth decrease is not due to the confinement but a common feature of the electrons on liquid ^{4}He because a very similar T dependence was observed in the threshold driving force (the Lorentz force) on bulk ^{4}He, that is, the threshold voltage [5,6] and the threshold magnetic field [14].

Shirahama and Kono considered that the decoupling occurs when the driving force ($-eE_{\parallel}$ in our case) exceeds the maximum restoring force produced by the combination of the shape of the DL and $eE_{\perp}$ [5]. They assumed, for simplicity, that the shape of the dimple is the same as the stationary one, which does not change during the decoupling process (rigid dimple model), and succeeded in explaining the dependence of their threshold voltage on some parameters. The threshold field $E_{\mathrm{rigid}}^{\mathrm{th}}$ calculated in this rigid dimple model is shown in Fig. 4. For the calculation, we use the fact that the shape of the DL in the stationary state is determined by the balance of the surface tension and the pressure from the electrons [15]. $E_{\mathrm{rigid}}^{\mathrm{th}}$ decreases with increasing T because of the shallowing of the dimple due to the thermal displacement of the electrons and jumps to zero at T_m^{2D} as a result of the sudden disappearance of the DL [16]. The calculated $E_{\mathrm{rigid}}^{\mathrm{th}}$ is several times smaller than the observed $E_{\parallel}^{\mathrm{th}}$.

The BC scattering, however, occurs before the decoupling, and thus, the WS should decouple from the DL that deepens due to the BC scattering. The decoupling including the deformation of the DL was discussed by Vinen with a simple hydrodynamic model [7]. He showed that, in the liquid with no damping, the depth should diverge as v approaches v_1, and therefore, the WS never decouples. In practice, damping such as the natural damping of ripplons exists in the liquid, which limits the dimple depth. The dimple depth and therefore the maximum restoring force produced by the deepened DL are inversely proportional to the damping parameter within the hydrodynamic calculation [7,17]. The observed enhancement of $E_{\parallel}^{\mathrm{th}}$ over $E_{\mathrm{rigid}}^{\mathrm{th}}$ in Fig. 4 strongly suggests that the decoupling actually occurs from the deepened DL. However, the increase in the depth is only on the order of $E_{\parallel}^{\mathrm{th}}/E_{\mathrm{rigid}}^{\mathrm{th}}$, and it is much smaller

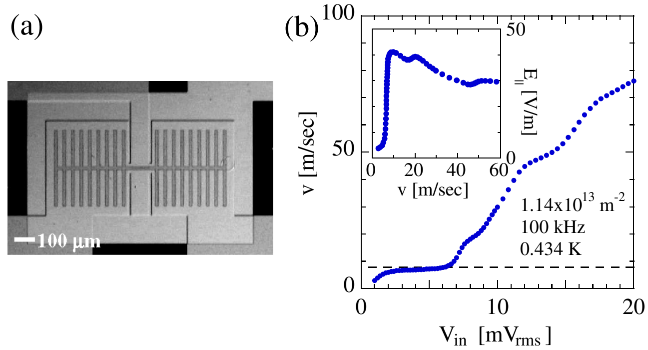

FIG. 5 (color online). (a) Device similar to that employed by Glasson *et al.* [10]. The center channel is 160 μm long and 15 μm wide. (b) v as a function of V_{in} obtained with this device. The dashed line indicates v_1. Inset: $E_{\parallel}$ as a function of v obtained by assuming the lumped-constant circuit [Fig. 1(d)] (see text).

than that expected from the extremely small natural damping of ripplons [18]. The damping also arises from the escape of the ripplons from the BC scattering area to outside. This may limit the dimple depth, but it cannot explain the gradual decrease in $E_{\parallel}^{\text{th}}$ as T approaches T_m^{2D}. Because $E_{\parallel}^{\text{th}}$ continuously vanishes at T_m^{2D}, the property of the WS seems to be involved in the decoupling mechanism.

Now, we compare our results with those reported by Glasson *et al.* for the 16 μm-wide channel [10]. They observed an oscillation of $E_{\parallel}$ as a function of v and attributed it to the dynamical ordering of the electrons into parallel filaments. However, our results (Fig. 3) are quite different from theirs despite the similar device used. The difference between both experiments is that their device has a much shorter center channel and a different pattern of the reservoir channels. To clarify the origin of this discrepancy, we also fabricated a similar pattern of channels as they employed [Fig. 5(a)]. v in the center channel obtained for this device is shown in Fig. 5(b). Note that v is deduced directly from I without the lumped-constant circuit analysis. v exhibits a stairlike increase with V_{in}, and this behavior is explained in terms of the BC scattering and decoupling transition as follows. The first plateau corresponds to the BC scattering-limited velocity in the center channel, as indicated by the dashed line in Fig. 5(b). With increasing V_{in}, the decoupling occurs in the center channel, followed by the BC scattering at the two innermost reservoir channels, resulting in the second plateau. Such successive BC scattering and decoupling in the reservoir channels cause the stairlike increase of v. If we calculate R, or namely $E_{\parallel}$, by assuming the lumped-constant circuit shown in Fig. 1(d) though the analysis with this circuit is not justified for the short center channel, we obtain an oscillating behavior in $E_{\parallel}$ as a function of v [inset of Fig. 5(b)], which is similar to that reported by Glasson *et al*. Thus, the oscillating behavior is not intrinsic but artificial.

In summary, we investigate the nonlinear transport of the WS in channels 8 and 15 μm in width. Owing to the uniform distributions of v and $E_{\parallel}$, we observe the BC scattering-limited velocity and the decoupling transition more clearly than any other experiments. Our results naturally explain the unusual nonlinearity reported by Glasson *et al.* by considering the geometry. Apart from this, the observed enhancement of $E_{\parallel}^{\text{th}}$ over $E_{\text{rigid}}^{\text{th}}$ directly indicates that the dimple depth dynamically increases due to the BC scattering and that the decoupling occurs from the deepened DL. However, the magnitude of $E_{\parallel}^{\text{th}}$ and its temperature dependence are not explained yet. Because the difficulties associated with the magnetic field and the inhomogeneity of v and $E_{\parallel}$ are removed, the obtained $E_{\parallel}^{\text{th}}$ should be unambiguously explained.

We thank Yu. P. Monarkha for helpful discussion. This work is partly supported by a Grant-in-Aid for Scientific Research from MEXT, Japan.

*hikegami@riken.jp

[1] *Two-Dimensional Electron Systems on Helium and Other Cryogenic Substrates*, edited by E. Y. Andrei (Kluwer Academic, Dordrecht, 1997).
[2] Y. P. Monarkha and K. Kono, *Two-Dimensional Coulomb Liquids and Solids* (Springer-Verlag, Berlin, 2004).
[3] A. Kristensen, K. Djerfi, P. Fozooni, M. J. Lea, P. J. Richardson, A. Santrich-Badal, A. Blackburn, and R. W. van der Heijden, Phys. Rev. Lett. **77**, 1350 (1996).
[4] M. I. Dykman and Y. G. Rubo, Phys. Rev. Lett. **78**, 4813 (1997).
[5] K. Shirahama and K. Kono, Phys. Rev. Lett. **74**, 781 (1995).
[6] K. Shirahama and K. Kono, J. Low Temp. Phys. **104**, 237 (1996).
[7] W. F. Vinen, J. Phys. Condens. Matter **11**, 9709 (1999).
[8] Y. G. Rubo and M. J. Lea, Physica (Amsterdam) **284-288B**, 1922 (2000).
[9] Y. P. Monarkha and K. Kono, Two-Dimensional Coulomb Liquids and Solids (Ref. [2]), Chap. 8.
[10] P. Glasson, V. Dotsenko, P. Fozooni, M. J. Lea, W. Bailey, G. Papageorgiou, S. E. Andresen, and A. Kristensen, Phys. Rev. Lett. **87**, 176802 (2001).
[11] H. Ikegami, H. Akimoto, and K. Kono, J. Low Temp. Phys. **150**, 224 (2008).
[12] H. Ikegami, H. Akimoto, and K. Kono (to be published).
[13] M. Saitoh, J. Phys. Soc. Jpn. **42**, 201 (1977).
[14] R. Giannetta and L. Wilen, Solid State Commun. **78**, 199 (1991).
[15] Y. P. Monarkha and V. B. Shikin, Sov. J. Low Temp. Phys. **9**, 471 (1983).
[16] C. C. Grimes and G. Adams, Phys. Rev. Lett. **42**, 795 (1979).
[17] Y. P. Monarkha and K. Kono, J. Phys. Soc. Jpn. **74**, 960 (2005).
[18] P. Roche, G. Deville, K. O. Keshishev, N. J. Appleyard, and F. I. B. Williams, Phys. Rev. Lett. **75**, 3316 (1995).